Available online at www.sciencedirect.com
ScienceDirect
Journal of Controlled Release 117 (2007) 238–245
journal of controlled release
www.elsevier.com/locate/jconrel

Assembled microneedle arrays enhance the transport of compounds varying over a large range of molecular weight across human dermatomed skin

F.J. Verbaan [a], S.M. Bal [a], D.J. van den Berg [a], W.H.H. Groenink [a], H. Verpoorten [a], R. Lüttge [b], J.A. Bouwstra [a,*]

[a] Department of Drug Delivery Technology, Leiden/Amsterdam Center for Drug Research, P.O. Box 9502, 2300 RA, Leiden, The Netherlands
[b] BIOS Lab-on-a-chip group, MESA+ Research Institute, University of Twente, P.O. Box 217, 7500 AE, Enschede, The Netherlands

Received 23 August 2006; accepted 6 November 2006
Available online 17 November 2006

Abstract

In this study, we demonstrate the feasibility to use microneedle arrays manufactured from commercially available 30G hypodermal needles to enhance the transport of compounds up to a molecular weight of 72 kDa.

Piercing of human dermatomed skin with microneedle arrays was studied by Trypan Blue staining on the SC side of the skin and transepidermal water loss measurements (TEWL). Passive transport studies were conducted with Cascade Blue (CB, Mw 538), Dextran–Cascade Blue (DCB, Mw 10 kDa), and FITC coupled Dextran (FITC-Dex, Mw 72 kDa). Microneedle arrays with needle lengths of 900, 700 and 550 μm are able to pierce dermatomed human skin as evident from (a) the appearance of blue spots on the dermal side of the skin after Trypan Blue treatment and (b) elevated TEWL levels after piercing compared to non-treated human dermatomed skin. Microneedles with a length of 300 μm did not pierce human skin in vitro. Transport studies performed with model compounds ranging from 538 Da to 72 kDa revealed that pretreatment with microneedle arrays enhanced the transport across dermatomed human skin. However, some degradation was also observed for FITC-Dex and DCB. We conclude that assembled microneedle arrays can be used to deliver compounds through the skin up to a molecular weight of at least 72 kDa.

Keywords: Microneedles; Transdermal drug delivery; Macromolecules; Skin

1. Introduction

Nowadays, there is a growing demand for the delivery of macromolecules, such as biopharmaceuticals [1], which are difficult to deliver by the oral route. An alternative delivery route is the transdermal route. However, a major problem in delivering drugs via the skin is the skin barrier, which is located in the outermost layer of the skin, the stratum corneum. A means to overcome the skin barrier is based on the formation of mechanically produced conduits through the stratum corneum by the use of an array of small needles, i.e. microneedles arrays [2–14]. Since the first publication by Henry et al. in 1998 [5], microfabrication techniques for the production of silicon, metal, glass and polymer microneedle arrays with micrometer dimensions have been described [13,15–17]. The microneedles can be either solid or hollow and can posses a plethora of geometries. The microfabrication of microneedles involves the use of tools developed by the microelectronic industry to make integrated circuits. Although these tools offer the potential for mass production of the microneedles, production is often highly specialized and includes complex multi-step processes [18,19]. Furthermore, silicon microneedle arrays are fragile, the use of silicon is relatively expensive, and silicon is yet unproven as a biocompatible material [20]. We therefore chose to use commercially available small 30G needles made from stainless steel. Metal is cheaper and stronger than silicon and furthermore, metal is biocompatible [21]. The needles are fixed on a backplate forming arrays having a needle length varying between 300 and 900 μm.

There already is a variety of literature reporting the transport enhancing properties of microneedle arrays. For instance, the

* Corresponding author. Tel.: +31 715274208; fax: +31 715274565.
E-mail address: Bouwstra@chem.leidenuniv.nl (J.A. Bouwstra).

0168-3659/$ - see front matter © 2006 Elsevier B.V. All rights reserved.
doi:10.1016/j.jconrel.2006.11.009

flux of small (i.e. <1000 Da) compounds like calcein [5], diclofenac [22], methyl nicotinate [23] and bischloroethyl nitrosourea [24] was increased by microneedle arrays. Successful application of microneedles to increase the transport of intermediate compounds (i.e. between 1 and 10 kDa) like FITC-Dextran [25], desmopressin [8] and insulin [9,13,16,22] was reported as well. In addition, microneedles also had a beneficial effect of the flux of large compounds (i.e. >10 kDa) like FITC-Dextran [25], bovine serum albumin [12], ovalbumin [26], antisense oligonucleotides [27], plasmid DNA [28] and nanospheres [10,29].

However, only limited information is available on the effect of microneedle arrays on the transport of compounds with varying molecular weight across the skin. In this paper, we systematically study the feasibility to use microneedle arrays varying in length between 300 and 900 μm for cutaneous delivery of low and high molecular weight compounds. Piercing of human dermatomed skin was studied by visual inspection and transepidermal water loss measurements. Transdermal transport of compounds with varying molecular weight between 538 Da and 72 kDa was studied using flow-through diffusion cells. The results of the present study show the feasibility of the assembled microneedle arrays to enhance the transport of low and high molecular weight compounds across the skin for microneedle lengths longer than 300 μm.

2. Materials and methods

2.1. Materials

Cascade Blue (CB, Mw 538) and Dextran–Cascade Blue (DCB, Mw 10 kDa) were purchased from Invitrogen (Breda, The Netherlands). Fluoresceinisothiocyanate coupled Dextran (FITC-Dex, Mw 72 kDa) was obtained from Sigma (Zwijndrecht, The Netherlands) as well as all other chemicals. 30G hypodermic needles were purchased from Becton and Dickinson (Alphen aan de Rijn, The Netherlands).

2.2. Microneedle array fabrication

Microneedle arrays were manufactured from commercially available 30G hypodermic needles (Fig. 1A and B). A polyetheretherketone mold (diameter 9 mm) was manufactured, in which a 4*4 pattern of holes was drilled (pitch 1.25 mm). The needles were placed through the holes at a predetermined length of 300, 550, 700 and 900 μm. Subsequently, the needles were cut and glued at the back of the mold. To facilitate the handling of the microneedle array, a manual applicator was designed in which the microneedle array can be precisely fixed.

2.3. Preparation of dermatomed human skin

Dermatomed human skin was prepared as described by Nugroho et al. [30]. In short, abdominal or breast skin was obtained from local hospitals following cosmetic surgery and was used within 24 h after surgery. Residual subcutaneous fat was removed using a surgical scalpel and the skin surface was carefully wiped with 70% ethanol and demiwater. The skin was fixed on a styrofoam support and the skin was dermatomed to a thickness of 300–400 μm using a Padgett Electro Dermatome Model B (Kansas City, USA). The skin was stored at −80 °C until use, except for transdermal transport studies where fresh human skin was used.

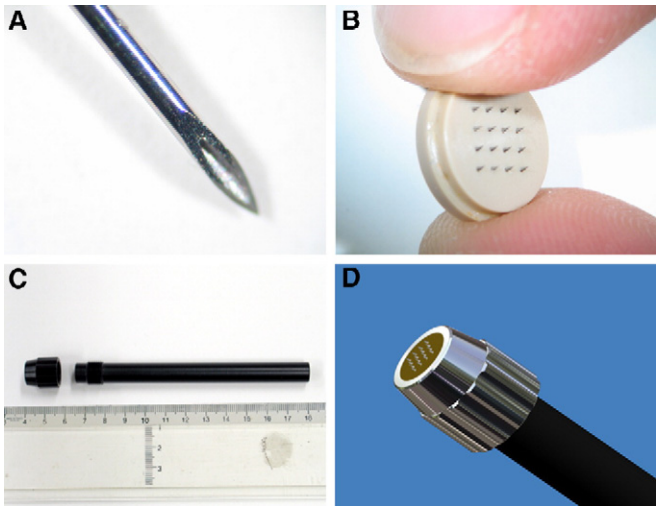

Fig. 1. The microneedle array consisting of commercially available needles and applicator to manually pierce the skin. (A) A picture of a 30G needle, (B) an angled view of a microneedle array. (C) Top view of the applicator with a ruler for comparison reasons, (D) A drawing of an angled view of the applicator.

2.4. Piercing of dermatomed human skin

Dermatomed human skin (DHS) was stretched on parafilm to counteract the elasticity of the skin after which disks of DHS (Ø 22 mm) were punched. Subsequently, the skin was supported by styrofoam to protect the microneedles from damage and pierced for 1 min using the manual applicator at approximately 50 N pressure.

2.5. Visual inspection of human dermatomed skin

Visualization studies were performed after the skin had been pierced with the applicator. The SC side of the pierced DHS was covered with 0.4% Trypan Blue dye in PBS for 1 h. The dye was then removed and the skin was evaluated for the appearance of blue dots on the dermal side of the DHS.

2.6. Cryo-scanning electron microscopy (Cryo-SEM)

Pieces of pierced DHS were mounted to a metal stub using OCT compound (Sakura, Tokyo, Japan) and subsequently fixed by plunge-freezing in liquid nitrogen. The frozen samples were transferred to a cryo-stage (Oxford Instruments CT 1500 HF, Eynsham, UK). The samples were shortly sublimated and subsequently sputter-coated with a layer of platinum. The samples were examined using a Cryo-SEM (Jeol 6300F FESEM, Tokyo, Japan).

2.7. Transepidermal water loss (TEWL) measurements in vitro

DHS was placed in a glass Franz cell, and the edges of the skin were coated with a multipurpose silicon water repellent (734, Dow Corning GmbH, Wiesbaden, Germany) to prevent the skin from drying out. The receiver compartment was filled with PBS (NaCl 8 mg/ml, Na_2HPO_4 2.86 mg/ml, KH_2PO_4 0. 2 mg/ml, KCl 0.19 mg/ml, pH 7.4). The TEWL values were measured with a Tewameter TM 210 (Courage+Khazaka, Köln, Germany). After placement of the probe on the top of the Franz cell, the TEWL values were recorded for 1 h in a climate room at room temperature and controlled humidity.

2.8. Diffusion studies

In vitro transport studies were performed as described by Grams et al. using continuous flow-through diffusion cells (PermeGear, Inc, Bethlehem, USA) [31]. The diffusion area was 1.16 cm^2. After piercing the DHS with microneedle arrays as described above, the pretreated DHS or control DHS was immediately placed between the donor compartment and receptor compartment with the SC side facing the donor compartment. A disk of wire gauze (Ø 18 mm) was used to support the DHS. The acceptor phase was PBS and was kept at 37 °C resulting in a skin temperature of 32 °C in the diffusion cell. The donor solutions contained 1 ml of either of CB, DCB or FITC-Dex (200 μM) in PBS. The flow rate of the PBS in the acceptor chamber was maintained at approximately 1 ml/h by a peristaltic pump (Ismatec SA, Glattbrugg, Switzerland). The donor compartment was covered with 3 M tape to establish occlusive conditions. Hourly fractions of the acceptor phase were collected over a period of 20 h and analyzed by HPLC.

2.9. Analysis by HPLC

The fluorescent intensity of CB and DCB was determined by injecting 100 μl of sample on a Waters HPLC system consisting of a Waters 600 controller coupled to a Waters 717 plus auto sampler and a Waters 474 Scanning Fluorescence Detector (Waters Chromatography B.V., Etten-Leur, The Netherlands). For both CB and CBD, excitation and emission wavelengths of 401 and 431 nm were used. PBS was used as the mobile phase at a flow rate of 1 ml/min. The fluorescent intensity of FITC-Dex samples was determined using a fluorimeter (Perkin Elmer LS50-B, Groningen, The Netherlands) at excitation and emission wavelengths of 492 and 518 nm.

2.10. Determination of intact compound in the donor and receiver fluids

In order to determine whether degradation of the probes occurs during the transport studies donor and receiver fractions were analyzed using size exclusion chromatography (SEC). After the transport study 250 μl of donor solution containing FITC-Dex was collected from the donor compartment and diluted 10 times to a final volume of 2.5 ml in PBS. The receiver fractions were pooled immediately after the transport study. The pooled receiver fluids were concentrated by freeze drying overnight and dissolved in 2.5 ml of demineralized water and subsequently applied on a PD10 column and eluted with demineralized water. For DCB, after the transport study 5 μl of donor solution was collected and diluted 500 times to a final volume of 2.5 ml in PBS. Receiver fluids were pooled and applied on a PD10 column. During SEC of both DCB and FITC-Dex, 1 ml fractions were collected with a fraction collector (Bromma 2212 Helirac, LKB, Sweden) after which the fractions were analyzed for fluorescence. Stock solutions of each compound were similarly treated and analyzed.

2.11. TEWL measurements in human volunteers

Four volunteers with healthy skin conditions between the age of 22 and 34 years participated in this study. Prior to all testing, the volunteers were asked to acclimate in a humidity and temperature controlled room 20 min prior to piercing. The volunteers were treated on the left volar forearm with assembled microneedles arrays using the manual applicator, after which the electrode was placed on the treated skin site and TEWL values were measured with a Tewameter TM 210 (Courage+Khazaka, Köln, Germany) during a period of 1 min. The assembled microneedle arrays were sterilized by immersion in 70% ethanol.

3. Results

3.1. Fabrication of microneedle arrays

The microneedle arrays consist of commercially available 30G hypodermic needles. An intact needle is depicted in Fig. 1A. The needles have an outer diameter of approximately 300 μm. The needles were placed in a 4*4 pattern into a mold and tailored to a length of 300, 550, 700 or 900 μm. In Fig. 1B, a typical example of a microneedle array is shown, with a microneedle length of 700 μm. The pitch of the microneedles is 1.25 mm, resulting in a microneedle array with a surface of 16.4 mm^2. A hand-held applicator was designed in which the abovementioned microneedle arrays were fixed (Fig. 1C and D) to facilitate reproducible puncturing of the dermatomed human skin by the microneedle array.

3.2. In vitro evaluation of piercing of human skin with microneedle arrays

To study the piercing of the microneedle arrays, Trypan Blue dye was applied to the SC side of the skin. The presence of conduits in the skin can be visualized by the appearance of blue dots at the dermal side. Fig. 2 shows that the microneedle arrays with microneedle lengths of 900, 700 and 550 μm form 4*4 pattern of blue dots. The appearance of blue dots was absent when dermatomed human skin was pierced with a microneedle array with a microneedle length of 300 μm. These results indicate that microneedles with microneedle lengths of 900, 700 and 550 μm have pierced the skin and created conduits for transport of the Trypan Blue dye across the skin. The intensity

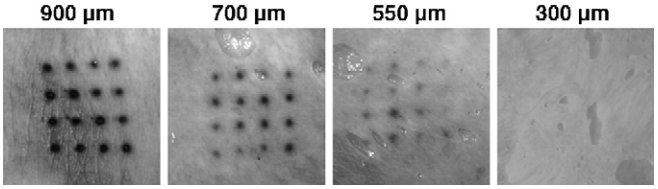

Fig. 2. Piercing of dermatomed human skin with arrays of microneedles having a length of 900, 700, 550 and 300 µm using the manual applicator as visualized with the Trypan Blue assay.

of the blue dots is stronger for the longer microneedles than for the shorter microneedles.

Fig. 3 shows a magnification of a conduit formed by piercing of human dermatomed skin with a microneedle array with a microneedle length of 550 µm. The SC side is facing upwards. A moon-shaped conduit with sharp edges is formed by the microneedle, caused by the shape of the tip of a 30G needle.

To quantify the piercing properties, TEWL values of dermatomed human skin in vitro were measured after microneedle treatment. Non-treated skin was used as a control. Skin punctured 6 times with an ordinary 30G hypodermic needle was used as a positive control. Fig. 4 shows a clear positive trend between the TEWL levels and the microneedle length, the 550 µm microneedles giving the lowest levels (about 9 g/h/m^2) and the 900 µm microneedles giving the highest TEWL levels (about 20 g/h/m^2). These values are clearly higher than the TEWL values of the control (about 2 g/h/m^2). The positive control resulted in sharply increased TEWL values of about 20 g/h/m^2. These results are in agreement with the results obtained from the visual inspection after incubation with the Trypan Blue dye. TEWL levels of microneedle-treated skin were always higher than the basal levels and sometimes approached the levels of the positive control.

3.3. Passive transport studies with compounds varying in molecular weight

In Fig. 5, the results of the in vitro transdermal transport studies using compounds varying in molecular weight, namely CB (Mw 538, Fig. 6A), DCB (Mw 10 kDa, Fig. 5B), and FITC-Dex (Mw 72 kDa, Fig. 5C) are presented. The transport of each compound was determined after pretreatment of the skin with microneedle arrays with a microneedle length of 550, 700 and 900 µm. For all compounds, the control skin (i.e. no microneedle array pretreatment) resulted in non-

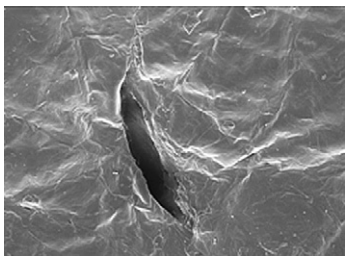

Fig. 3. Cryo-SEM of pretreated dermatomed human skin viewed from the SC side of the skin after piercing with a 550 µm microneedle array.

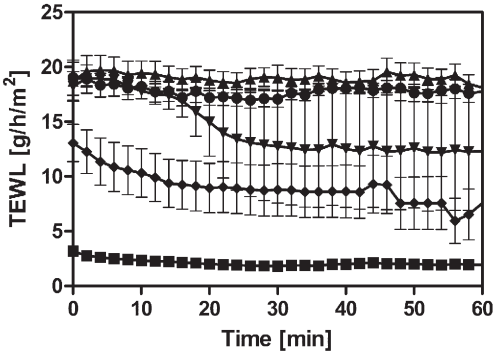

Fig. 4. Transepidermal water loss (TEWL) of dermatomed human skin pierced with microneedles arrays containing microneedles of different lengths using the hand-held applicator. Data are presented as averages±SEM, $n=3$ of three donors. Upward triangles: positive control, circles: 900 µm microneedle arrays, downward triangles: 700 µm microneedle arrays, diamonds: 550 µm microneedle arrays, squares: untreated skin.

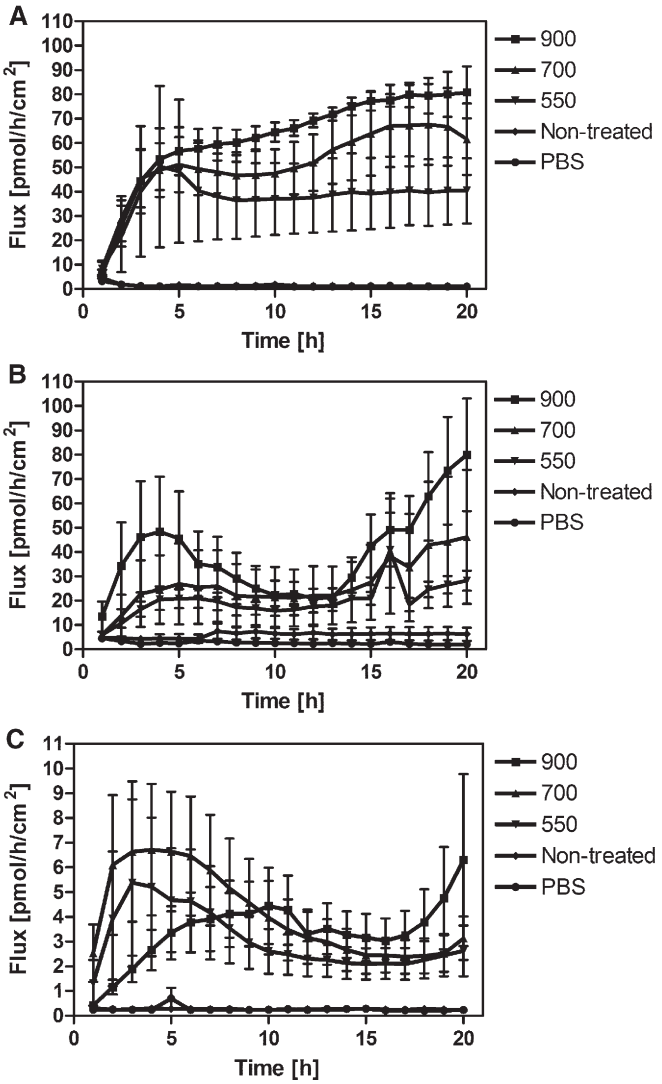

Fig. 5. Transport of compounds with different molecular weights after pretreatment of dermatomed human skin with microneedle arrays using the conventional applicator. (A) Cascade Blue Mw 538, (B) Cascade Blue–Dextran Mw 10 kDa, (C) FITC-Dextran Mw 72 kDa. Data are presented as averages± SEM, $n=6$ of three donors.

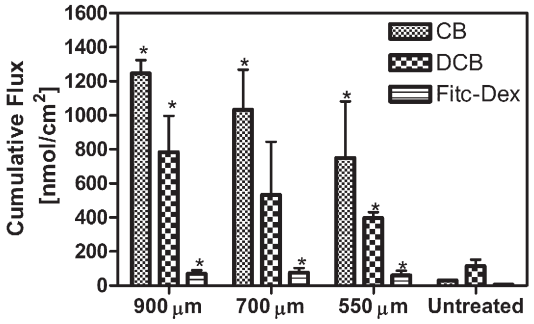

Fig. 6. Total accumulated amount of compounds with different molecular weights after pretreatment of dermatomed human skin with microneedle arrays using the conventional applicator transported across the skin. Data are presented as averages±SEM, $n=6$ of three donors. *: $P<0.05$.

detectable fluxes, except for the DCB compound: a very small flux was observed. For all compounds and microneedle lengths, pretreatment with microneedle arrays resulted in a drastic increase in transport of the compound across dermatomed human skin compared to no pretreatment. After microneedle array pretreatment, in the initial period of the diffusion experiment there is a gradual increase in transport for all three compounds, while after 4–5 h the transport rate sometimes reduces. This might be due to swelling of the SC reducing the size of the conduits. At the end of the diffusion period, often an increase in flux was observed. The reason for this is not clear, but might be because of some damage of the skin surrounding the conduits. Furthermore, the transport rate of the largest MW compound (FITC-Dex) is much lower than the fluxes observed for CB and for DCB, but is still significantly increased compared to the transport rate of control skin.

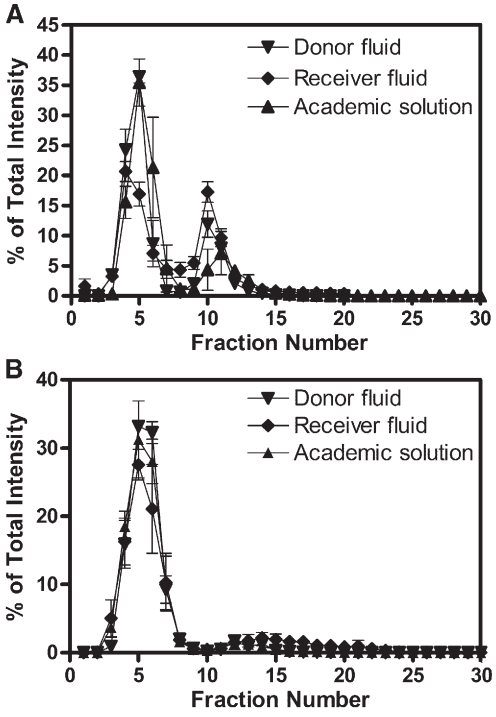

Fig. 7. Size exclusion chromatography of donor and receiver fluids from a transport experiment and academic solutions of (A) Cascade Blue–Dextran (Mw 10 kDa) or (B) FITC-Dextran (Mw 72 kDa) after pretreatment of dermatomed human skin with microneedle arrays using the manual applicator. Data are presented as averages±SEM, $n=3$.

Table 1
Calculated AUCs of the degradation peak after size exclusion chromatography of donor and acceptor fluids after a transport study with DCB and FITC-Dex

Compound	Fraction	Donor fluid	Acceptor fluid	Academic solution
DCB	Fraction 3–8	74.2 (±0.9)	56.6 (±7.0)	78.4 (±8.6)
	Fraction 9–13	24.8 (±0.9)	56.6 (±5.6)	19.3 (±8.9)
FITC-Dex	Fraction 3–8	93.6 (±0.8)	79.4 (±12.6)	95.5 (±0.9)
	Fraction 9–13	4.8 (±2.6)	9.6 (±6.5)	2.0 (±0.4)

The total accumulated amount of the compound transported across the skin after 20 h is provided in Fig. 6. There is no significant difference in total cumulative amounts between the various microneedle lengths, although a trend is observed that larger microneedle lengths resulted in a higher transport of CB and DCB. For all microneedle lengths, after 20 h the cumulative amounts are significantly higher than for the untreated situation ($P<0.05$), except for DCB after pretreatment with 700 μm microneedles ($P=0.08$). Degradation of the DCB and the FITC-Dex compounds in the donor and receiver fluids was also studied immediately after the diffusion experiments when skin was treated with microneedles as these molecules might shed their label during transport across the skin. Size exclusion chromatography of the receiver fluids revealed that the majority of the applied conjugates were transported through the skin intact, as shown in Fig. 7. To quantitatively assess the degradation, the area under the curve (AUC) of the degradation peak (i.e. fractions 9–13 eluting of the size exclusion column) in the chromatogram was calculated for both compounds. Table 1 summarizes the AUC of both compounds after transport. As a comparison, the AUC of a control solution of DCB and FITC-Dex was also calculated. For both studied compounds, the AUC in the donor fluids resembled the AUC observed in the control solutions. In contrast, the AUC observed in the acceptor fluid is significantly higher for DCB, but not for FITC-Dex. It should be noted, however, that the AUC of the degradation peak of DCB may be overrated because of the higher fluorescence intensity of CB (shed of label) compared to DCB (intact compound).

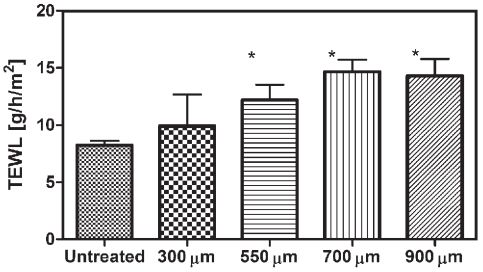

Fig. 8. Transepidermal water loss in humans after treatment with assembled microneedle arrays containing microneedles of different lengths using the using the hand-held applicator. Data are presented as averages±SD. *: $P<0.05$.

3.4. TEWL measurements in human volunteers

Four healthy volunteers were treated on the left fore arm with sterilized microneedle arrays for 1 min after which TEWL values were measured. Treatment with assembled microneedle arrays with a needle length of 900, 700 or 550 μm resulted, in significantly elevated TEWL levels compared to the untreated situation (Fig. 8). Assembled microneedle arrays with a needle length of 300 μm did not result in significantly increased TEWL levels compared to the untreated situation. A small trend is observed that long microneedle lengths give higher TEWL values compared to smaller microneedle lengths.

4. Discussion

In this study, we demonstrated the use of assembled microneedle arrays for delivery of high molecular weight compounds. We selected commercially available small 30G needles as a basis to produce mechanically assembled microneedle arrays. Metal needles are strong and are not buckled or damaged easily, and therefore have the ability to be reused in in vitro studies.

We designed a first set of experiments to determine whether the microneedle arrays pierce the skin. Visual inspection of pierced dermatomed skin (300–400 μm thick) showed that non-damaged tips of the microneedle protruded the skin for both the 900 and 700 μm microneedles, and no tips of microneedles could be visualized after piercing of the 550 μm microneedles (data not shown). The piercing properties of the microneedle arrays were confirmed by application of the Trypan Blue dye on the SC side of the skin, and subsequent appearance of blue dots on the dermal side of the skin for the 550, 700 and 900 μm microneedle arrays. These results indicate that the dye permeates into the skin more easily at sites where conduits are formed by the microneedles. Microneedle arrays with a needle length of 300 μm were not able to pierce the skin. We postulate that microneedles of sufficient length are required to overcome the bulk elastic tissue compression of the skin, after which the microneedles are able to rupture and penetrate the skin. In line with our results, Martanto et al. described very recently that human cadaver skin was indented when microneedles were inserted slowly into the skin [32]. It must be noted that in our study dermatomed human skin was used with a thickness of 300–400 μm. In our experience, the use of thinner and less flexible epidermal sheets facilitates the successful piercing with microneedles. This might be one of the reasons that other groups are able to use microneedles shorter than 300 μm [5,10,17] when manually piercing the skin.

To quantify the reduction in the skin barrier after pretreatment of microneedles, TEWL levels of pretreated skin were also measured. Elevated TEWL levels were observed compared to non-treated human dermatomed skin. There was a positive trend between the TEWL levels and the microneedle length, the 550 μm microneedle treatment results in elevated but low TEWL levels compared to the 900 μm microneedle treatment providing much higher TEWL levels. Assuming that the complete length of the microneedle is inserted into the skin, the tapered shape of the tip of the 30G needle, which is approximately 1 mm in length, is expected to result in the formation of conduits with different diameters, the shortest microneedles resulting in conduits with a smaller diameter. Obviously, TEWL levels are higher for conduits with larger diameters. To verify whether the dermatomed skin model has predictive value to the in vivo situation, a proof of concept study was performed in man where we measured TEWL levels after piercing with microneedle arrays. Importantly, short (i.e. 300 μm) microneedles did not result in successful piercing. A similar trend to the in vitro situation was observed, indicating that the in vitro dermatomed skin model has predictive value for the in vivo situation.

A means to improve the piercing of skin and create the possibility to use shorter microneedles is the design of an impact insertion system that pierces the skin with a certain speed. The design of applicators to increase the speed of microneedle insertion into the skin will be subject of further studies.

Although it is clear that the increase in TEWL levels is a result of pierced skin, it is not a predictive value for the transport of drugs across the skin, which is in line with the data presented by Chilcott et al. [33]. We therefore determined whether microneedle pretreatment also resulted in an increased transport of model compounds with increasing molecular weight up to 72 kDa. These compounds were chosen in order to determine whether a threshold of increased transport can be observed when increasing the molecular weight of the compound. This is of interest as there is an increasing demand for the delivery of large molecules such as antibodies and antigens across the skin. Importantly, the fluxes of all compounds are significantly higher than the controls, indicating that the molecular cut-off after microneedle array pretreatment is higher than 72 kDa, which is in line with the results presented by Wu et al. [25]. However, there is no significant difference in fluxes between the various microneedle lengths observed with the model compounds, although a trend is observed that larger microneedle lengths resulted in a higher transport of CB and DCB. Widera et al. also reported that the magnitude of antibody responses followed by intracutaneous administration of ovalbumin by a coated microneedle array patch system in mice was not significantly different for the three studied microneedle length designs (i.e. 225, 400 and 600 μm) [34]. Our studies indicate that, not only for the high molecular compounds, but also for the low molecular compounds, the length of the microneedles does not affect the transport enhancing properties of the microneedle arrays as long as the microneedles are long enough to penetrate the skin.

The degradation of compounds when transported across the skin is another issue not often addressed in the microneedle field. We show that degradation was limited for FITC-Dex, but was significantly present for DCB. However, the majority of DCB was transported intact over the skin. Interestingly, degradation was observed mainly in the receiver fluids. This result indicates that degradation occurs after being transported over the SC. Abla et al. recently reported a similar phenomenon which they contributed to the enzymatic degradation of peptides after transport over the SC using iontophoresis [35].

As a large MW compound (FITC-Dex) can be transported after pretreatment of microneedle arrays, this opens up the opportunity to deliver antigens to the skin, which is an attractive route for the development of protective immunization. Underneath the SC, in the epidermis the Langerhans cells are located, which are important for initiating an immune response. The Langerhans cells are located in the epidermis. Targeting the piercing of the microneedles to specific tissue layers like the epidermis is therefore an important issue and will be subject of future studies.

5. Conclusion

As evident from (a) the appearance of blue spots after Trypan Blue application and (b) elevated TEWL values, microneedles form conduits in the skin. This is observed both in vitro and in vivo. Passive transport studies with compounds varying in molecular weight indicate that the piercing of skin increases the flux of low and high molecular weight compounds. However, the length of the microneedles – as long as the microneedles are piercing the skin – does not dramatically change the penetration of the low and high molecular weight compounds.

Acknowledgments

This work is financially supported by the Dutch Technology Foundation (STW), project number LPG.5950.

References

[1] D.J. Crommelin, G. Storm, R. Verrijk, L. de Leede, W. Jiskoot, W.E. Hennink, Shifting paradigms: biopharmaceuticals versus low molecular weight drugs, Int. J. Pharm. 266 (1–2) (2003) 3–16.
[2] M.R. Prausnitz, Microneedles for transdermal drug delivery, Adv. Drug Deliv. Rev. 56 (5) (2004) 581–587.
[3] S.L. Tao, T.A. Desai, Microfabricated drug delivery systems: from particles to pores, Adv. Drug Deliv. Rev. 55 (3) (2003) 315–328.
[4] S. Kaushik, A.H. Hord, D.D. Denson, D.V. McAllister, S. Smitra, M.G. Allen, M.R. Prausnitz, Lack of pain associated with microfabricated microneedles, Anesth. Analg. 92 (2) (2001) 502–504.
[5] S. Henry, D.V. McAllister, M.G. Allen, M.R. Prausnitz, Microfabricated microneedles: a novel approach to transdermal drug delivery, J. Pharm. Sci. 87 (8) (1998) 922–925.
[6] S. Henry, D.V. McAllister, M.G. Allen, M.R. Prausnitz, Microfabricated microneedles: a novel approach to transdermal drug delivery, J. Pharm. Sci. 88 (9) (1999) 948.
[7] B.W. Barry, Novel mechanisms and devices to enable successful transdermal drug delivery, Eur. J. Pharm. Sci. 14 (2) (2001) 101–114.
[8] M. Cormier, B. Johnson, M. Ameri, K. Nyam, L. Libiran, D.D. Zhang, P. Daddona, Transdermal delivery of desmopressin using a coated microneedle array patch system, J. Control. Release 97 (3) (2004) 503–511.
[9] W. Martanto, S.P. Davis, N.R. Holiday, J. Wang, H.S. Gill, M.R. Prausnitz, Transdermal delivery of insulin using microneedles in vivo, Pharm. Res. 21 (6) (2004) 947–952.
[10] F. Chabri, K. Bouris, T. Jones, D. Barrow, A. Hann, C. Allender, K. Brain, J. Birchall, Microfabricated silicon microneedles for nonviral cutaneous gene delivery, Br. J. Dermatol. 150 (5) (2004) 869–877.
[11] W. Martanto, J.S. Moore, O. Kashlan, R. Kamath, P.M. Wang, M. O'Neal J, M.R. Prausnitz, Microinfusion using hollow microneedles, Pharm. Res. 23 (1) (2006) 104–113.
[12] J.H. Park, M.G. Allen, M.R. Prausnitz, Biodegradable polymer microneedles: fabrication, mechanics and transdermal drug delivery, J. Control. Release 104 (1) (2005) 51–66.
[13] M.A. Teo, C. Shearwood, K.C. Ng, J. Lu, S. Moochhala, In vitro and in vivo characterization of MEMS microneedles, Biomed. Microdevices 7 (1) (2005) 47–52.
[14] J.C. Birchall, Microneedle array technology: the time is right but is the science ready? Expert. Rev. Med. Devices 3 (1) (2006) 1–4.
[15] J.H. Park, M.G. Allen, M.R. Prausnitz, Polymer microneedles for controlled-release drug delivery, Pharm. Res. 23 (5) (2006) 1008–1019.
[16] S.P. Davis, W. Martanto, M.G. Allen, M.R. Prausnitz, Hollow metal microneedles for insulin delivery to diabetic rats, IEEE Trans. Biomed. Eng. 52 (5) (2005) 909–915.
[17] D.V. McAllister, P.M. Wang, S.P. Davis, J.H. Park, P.J. Canatella, M.G. Allen, M.R. Prausnitz, S. Kaushik, A.H. Hord, D.D. Denson, S. Smitra, S. Henry, Microfabricated needles for transdermal delivery of macromolecules and nanoparticles: fabrication methods and transport studies, Proc. Natl. Acad. Sci. U. S. A. 100 (24) (2003) 13755–13760.
[18] B. Ziaie, A. Baldi, M. Lei, Y. Gu, R.A. Siegel, Hard and soft micromachining for BioMEMS: review of techniques and examples of applications in microfluidics and drug delivery, Adv. Drug Deliv. Rev. 56 (2) (2004) 145.
[19] S. Zafar Razzacki, P.K. Thwar, M. Yang, V.M. Ugaz, M.A. Burns, Integrated microsystems for controlled drug delivery, Adv. Drug Deliv. Rev. 56 (2) (2004) 185.
[20] W.R. Runyan, K.E. Bean, Semiconductor Integrated Circuit Processing Technology, Addison-Wesley, New York, 1990.
[21] J.H. Braybrook, Biocompatiblity: Assessment of Medical Devices and Materials, Wiley, New York, 1997.
[22] H.J.G.E. Gardeniers, R. Luttge, E.J.W. Berenschot, M.J. de Boer, S.Y. Yeshurun, M. Hefetz, R. van 't Oever, A. van den Berg, Silicon micromachined hollow microneedles for transdermal liquid transport, J. Microelectromech. Syst. 12 (6) (2003) 855–862.
[23] R.K. Sivamani, B. Stoeber, G.C. Wu, H. Zhai, D. Liepmann, H. Maibach, Clinical microneedle injection of methyl nicotinate: stratum corneum penetration, Skin Res. Technol. 11 (2) (2005) 152–156.
[24] Y. Li, R.S. Shawgo, B. Tyler, P.T. Henderson, J.S. Vogel, A. Rosenberg, P.B. Storm, R. Langer, H. Brem, M.J. Cima, In vivo release from a drug delivery MEMS device, J. Control. Release 100 (2) (2004) 211–219.
[25] X.M. Wu, H. Todo, K. Sugibayashi, Effects of pretreatment of needle puncture and sandpaper abrasion on the in vitro skin permeation of fluorescein isothiocyanate (FITC)-dextran, Int. J. Pharm. 316 (1–2) (2006) 102–108.
[26] J.A. Matriano, M. Cormier, J. Johnson, W.A. Young, M. Buttery, K. Nyam, P.E. Daddona, Macroflux microprojection array patch technology: a new and efficient approach for intracutaneous immunization, Pharm. Res. 19 (1) (2002) 63–70.
[27] W. Lin, M. Cormier, A. Samiee, A. Griffin, B. Johnson, C.L. Teng, G.E. Hardee, P.E. Daddona, Transdermal delivery of antisense oligonucleotides with microprojection patch (Macroflux) technology, Pharm. Res. 18 (12) (2001) 1789–1793.
[28] J.A. Mikszta, J.B. Alarcon, J.M. Brittingham, D.E. Sutter, R.J. Pettis, N.G. Harvey, Improved genetic immunization via micromechanical disruption of skin-barrier function and targeted epidermal delivery, Nat. Med. 8 (4) (2002) 415–419.
[29] D.V. McAllister, P.M. Wang, S.P. Davis, J.H. Park, P.J. Canatella, M.G. Allen, M.R. Prausnitz, Microfabricated needles for transdermal delivery of macromolecules and nanoparticles: fabrication methods and transport studies, Proc. Natl. Acad. Sci. U. S. A. 100 (24) (2003) 13755–13760.
[30] A.K. Nugroho, G.L. Li, M. Danhof, J.A. Bouwstra, Transdermal iontophoresis of rotigotine across human stratum corneum in vitro: influence of pH and NaCl concentration, Pharm. Res. 21 (5) (2004) 844–850.
[31] Y.Y. Grams, J.A. Bouwstra, Penetration and distribution of three lipophilic probes in vitro in human skin focusing on the hair follicle, J. Control. Release 83 (2) (2002) 253–262.
[32] W. Martanto, J.S. Moore, T. Couse, M.R. Prausnitz, Mechanism of fluid infusion during microneedle insertion and retraction, J. Control. Release 112 (3) (2006) 357–361.

[33] R.P. Chilcott, C.H. Dalton, A.J. Emmanuel, C.E. Allen, S.T. Bradley, Transepidermal water loss does not correlate with skin barrier function in vitro, J. Invest. Dermatol. 118 (5) (2002) 871–875.
[34] G. Widera, J. Johnson, L. Kim, L. Libiran, K. Nyam, P.E. Daddona, M. Cormier, Effect of delivery parameters on immunization to ovalbumin following intracutaneous administration by a coated microneedle array patch system, Vaccine 24 (10) (2006) 1653–1664.
[35] N. Abla, A. Naik, R.H. Guy, Y.N. Kalia, Effect of charge and molecular weight on transdermal peptide delivery by iontophoresis, Pharm. Res. 22 (12) (2005) 2069–2078.